Universitas Carolina Pragensis

Facultas Mathematica Physicaque

Abstract of Doctoral Thesis

Fakulta Matematicko-fyzikální, Univerzita Karlova
Praha, Ceská Republika

&

Fyziologický ústav Akademie ved Ceské republiky Ceské Republiky

Transport zprostredkovaný odprahujícím proteinem-1 (UCP1) a jeho mutanty

Autoreferát doktorské disertacní práce

Eva Urbánková

Obor
F4 – Fyzika molekulárních a biologických struktur
Praha 2002

Faculty of Mathematics and Physics, Charles Universtiy
Prague, Czech Republic

&

Institute of Physiology, Academy of Sciences of the Czech Republic

The transport mediated by wild type and mutants of uncoupling protein 1 (UCP1)

Summary of Ph.D. Thesis

Eva Urbánková

Branch
F4 – Physics of molecular and biological structures
Prague 2002

Výsledky této disertacní práce byly získány behem doktorandského studia na Matematicko-fyzikální fakulte Univerzity Karlovy v Praze v letech 1997-2002.

Uchazec: **Mgr. Eva Urbánková**
Fyziologický ústav AV CR
Vídenská 1083, 142 20 Praha 4-Krc

Školitel: **RNDr. Petr Ježek, DrSc.**
Fyziologický ústav AV CR
Vídenská 1083, 142 20 Praha 4-Krc

Konzultant:

Školící pracovište: **Fyziologický ústav AV CR**
Vídenská 1083, 142 20 Praha 4-Krc

Oponenti: **Doc. RNDr. Dana Gášková, CSc.**
Fyzikální ústav UK, Matematicko fyzikální fakulta
Ke Karlovu 5, 121 16 Praha 2

RNDr. Jan Krušek, CSc
Fyziologický ústav AV CR
Vídenská 1083, 142 20 Praha 4-Krc

Autoreferát byl rozeslán dne:
Obhajoba se koná dne v hod. pred komisí pro obhajoby disertacních prací v oboru F4-Fyzika molekulárních a biologických struktur na MFF UK, Ke Karlovu 3, 120 00 Praha 2, v zasedací místnosti c. 105.

S disertacní prací se lze seznámit na Útvaru doktorandského studia MFF UK, Ke Karlovu 3, Praha 2.

Predseda oborové rady F4: **Doc. RNDr. Otakar Jelínek, CSc.**

INTRODUCTION

Mitochondria have been attracting attention of scientists for many decades. Recently, new themes have emerged - apoptosis, 'mitochondrial diseases' and their genetics, relations of mitochondria to several other diseases (e.g. diabetes mellitus), aging and regulation of body weight [45], [46]. One of the extensively developing topics is the research on mitochondrial uncoupling proteins.

Uncoupling proteins form a subfamily of mitochondrial anion carrier protein family (MACP). The best understood is the originally known, UCP1. It is expressed exclusively in the brown adipose tissue of mammals and has been proved to uncouple mitochondria by enabling proton back-flux into the mitochondrial matrix. The function of other uncoupling proteins, UCP2-5 (and PUMP, plant uncoupling mitochondrial protein) is not understood so well. Although these proteins are proposed to be involved in various physiological and patophysiological phenomena, such as thermoregulation, fever, regulation of body weight, regulation of radical oxygen species formation, apoptosis, diabetes mellitus type II etc., current knowledge about their function is limited and there is a lot of controversy in the field. The recent results suggest that most probably even UCP2-5 uncouple mitochondria in a similar way, as does UCP1.

The other question concerns the mechanism of uncoupling function of UCPs. Even for UCP1, there is still no consensus how this protein really functions. There are two incompatible hypotheses describing the uncoupling mechanism.

In my work, I have concentrated to several aspects of UCP1-mediated transport:

First, we took advantage of known sequences of UCP1-5 and searched for aminoacid residues, which are conserved among UCPs, but don't exist in other related proteins [25].

(2.) In the second step, a few of these residues were mutated and the proton and chloride transport was studied in the resulted mutants.

(3.) In order to introduce a new method suitable for studying UCP-mediated transport, I developed a reconstitution of UCP1 into planar lipid bilayers and measured basic properties of such a system. This part of the work was done in collaboration with Dr. Elena E. Pohl from Humboldt university, Berlin and Dr. Peter Pohl, Forschungsinstitut für Molekuläre Pharmakologie, Berlin.

(4.) I have participated in the project aimed to detect UCP2 and/or UCP3 in mitochondria isolated from various tissues. The methods developed involved measurements of the mitochondrial membrane potential, mitochondrial respiration and evaluation of nucleotide binding to intact mitochondria. Some of the results are shown in this work.

Uncoupling of mitochondria

According Mitchell's chemiosmotic theory [33], respiration chain in mitochondria creates proton electrochemical potential gradient,

$$\textbf{Eq. 1} \quad \Delta\tilde{m}_{H^+} = \Delta\Psi - \frac{2.3RT}{F}\Delta pH$$

which is then used by F_1F_0ATPase to synthetize ATP and also to transport many kinds of metabolites to mitochondria (e.g. ADP/ATP antiport, phosphate import etc.).

When an uncoupler is added to mitochondria, it enables protons to get back to matrix and dissipates the proton electrochemical potential. The result is the fall of ? μ_{H+} and the production of heat. There are synthetic uncouplers (dinitrophenol, FCCP, CCCP) as well as natural ones - uncoupling proteins (UCPs). Fatty acids (FAs) are required for the uncoupling mediated by UCPs. Except of uncoupling proteins, for those uncoupling is their main function (this is known at least for UCP1), some other proteins also may uncouple mitochondria at certain conditions.

Mitochondrial anion carrier protein (MACP) family

Mitochondria require for their function not only proteins of the electron transport chain and the F_1F_0 ATP synthase, but also numerous other membrane proteins that facilitate the traffic of the substrates, ions and proteins required in the mitochondrial matrix. The inner membrane represents the only barrier for membrane-impermeable molecules. Proteins capable to translocate anions across the inner mitochondrial membrane form a gene family ("MACP family"). Uncoupling caused by fatty acids is not taking place exclusively in BAT mitochondria, where UCP1 is present. Other mitochondria are also uncoupled by FAs and it is supposed that other MACPs are also capable to exert fatty-acid induced uncouping.

Uncoupling proteins

There were five sequences of uncoupling proteins found in the human genome (all of them are found also in genomes of other mammals and some of them also in other kinds of vertebrates and invertebrates) and three in the *Arabidopsis thaliana* genome [17]. The first known uncoupling protein, UCP1, was found in mitochondria of brown adipose tissue (BAT). Its properties were known already from the studies on the whole mitochondria - proton back flux induced by fatty acids and binding of purine nucleotides, that inhibit the proton transport. The UCP1-enabled proton flux causes, that BAT mitochondria are uncoupled and produce heat, unless purine nucleotides are present. UCP2 is known to be expressed in all kinds of tissues studied [28], [34] and was suggested to be involved in diabetes mellitus (type II), apoptosis, fever, body weight regulation and defence against reactive oxygen species [69]. UCP3 is skeletal-muscle-specific [5] and supposed to enable muscle thermogenesis [69], [5]. Brain-specific UCP4 [32] and BMCP1 (or UCP5) [43] were discovered. An UCP4-like protein seems to be the ancestral protein to UCP subfamily [17].

There are two theories trying to explain the UCP1 function - fatty acid cycling theory [48] and fatty acid buffering theory [14]. According the first one, UCP1 has one transport pathway for various anions. Protons are not transported by UCP1 itself, but when FAs are present in the membrane, UCP1 transports FA anions and protonated FAs return via flip-flop. When they release protons, the cycle is closed (see Figure 1 for more detailed explanation). According the FA buffering model, FAs (in an unknown stoichiometry) bind to UCP1 and provide a 'missing' carboxyl group(s) along the proton translocation path [14].

Support for FA cycling (the reasons are ordered from more abstract to more concrete):

- UCP1 belongs genetically to the family of anion carriers and is indeed known to transport various anions [23], [19].
- UCP1 is known to transport alkylsulfonates (more hydrophobic more easily), which are very similar to FAs, but their pK is much lower. Therefore they are not activating proton transport. However, when propranolol is present (enables to the complex alkylsulfonate-H to get back), proton transport is observed [18].
- Alkylsulfonates competitively inhibit FA-induced proton transport. Cl^- transport is competitively inhibited by alkylsulfonates and fatty acids [24], suggesting that only one transport pathway exists in UCP1 for FAs and other anions.
- FAs which are not able to flip-flop (acidify liposome interior) were not activating UCP1-mediated proton transport [21],[22].

Support for FA buffering

- Analogy with other H^+ transporters, which contain an array of carboxyl groups facilitating the H^+ transfer along the chain of water molecules [29]. Bound FAs could provide some of these groups.
- Much lower rate for Cl^- transport than for H^+ transport (~10x difference) [29].

- Existence of the mutant (E167Q), which is not able to transport Cl^-, but H^+ transport exerted by it is retained.[9]

Figure 1 Fatty acid cycling provided by UCP1. When FA anions are transported by UCP1 through the membrane, some of them become protonated (in order to retain the equilibrium between FA^- and FA.H). Some of FA.H then flip-flop to the other side of the membrane (in order to retain equilibrium of FA.H between the two lipid sheets of the membrane). Some of FA.H then deprotonate on the other side and thus, protons are transported.

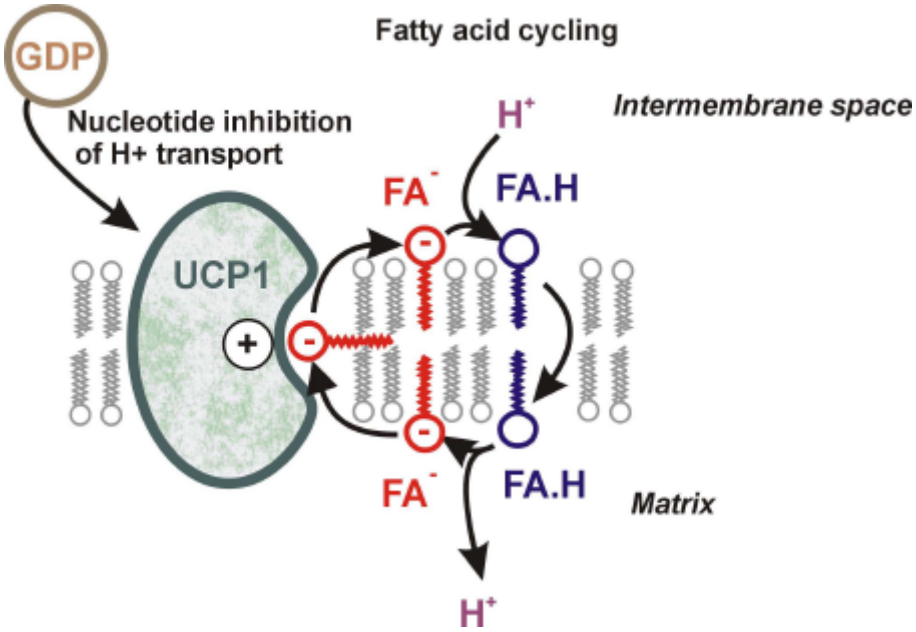

It seems that FA cycling gives scientifically 'smarter' explanation and is supported more strongly by experimental results, but it has to wait for its final proof.

THEORETICAL PART: UNCOUPLING PROTEIN FAMILY - COMPARISON OF SEQUENCES

We made an attempt to get as much as possible from analysis of UCP sequences. Main part of this approach laid in aligning known sequences of UCP's and their nearest relatives.

In order to predict common functional domains within the UCP subfamily, we have screened accessible UCP sequences and searched for similar sequence motifs that are unique just for UCPs within the MACP gene family. If a residue is common for UCPs and is not present in other MACPs, there is a probability, that it is involved directly in the UCP function (i.e. H^+ uniport induced by fatty acids, transport of various anions and inhibition of this transport by purine nucleotides).

Some other carriers of the family were also shown to provide FA-induced uncoupling (inhibited not by PN, but by their specific inhibitors), but it is never the main function of these carriers and it is probably much weaker than UCP-provided uncoupling.

The matrix UCP-specific sequence does not appear in BMCP1.

The connecting matrix segments of UCPs always begin by the major part of the MACP signature sequence [1],[49],[50],[35]. One may speculate that this sequence predetermines the termination of the odd transmembrane segments and the formation of the matrix segments in all MACPs. Searching for the UCP-specific sequence motifs, we found first such a motif, specific for UCP-subfamily except of BMCP1, in the 2nd matrix segment. This UCP-specific sequence motif, an "UCP-signature", starts with Arg152 of UCP1 and its consensus sequence can be written as follows:

[+]- f**-X-Gly/Ser-Thr/n-X-NH/[–]-Ala-**f

where [+](or [–]) stands for positively (negatively) charged residues; n is a nonpolar nonaromatic residue; ϕ is an aromatic residue; NH represents Asn or His. The whole matrix UCP signature is not contained in BMCP1 and in any of the MACPs of mammalian or yeast origin. But, its Arg pair and two Tyr exist in the yeast dicarboxylate transporter (DTP), while the last 7-residue motif exists in the YIA6 and YEA6 yeast carriers. In the following part of the 2nd matrix segment, Ile163 and Glu167 are conserved in UCPs and some MACPs.

UCP-signatures in transmembrane segments

The 1st UCP-specific motif appears to be the 8-residue motif preceding the MACP signature in the 1st transmembrane segment. It starts with Ala23:

Ala/Ser-Cys/Thr/n-n/Phe-Ala/Gly-[–]-n/Phe-n/Cys-Thr-Phe/n.

With alternative first Ser, second Ile and Phe after Glu, this signature is valid also for BMCP1. The 2nd transmembrane UCP signature can be described as follows:

Gly/Ala-Ile/Leu-Gln/X-[+]-NH-n/Cys-Ser/n-f**/X-n/Ser-OH/Gly-n-[+]-Ile/Met-Gly/Val-n/Thr**,

starting at Gly80 of UCP1, where [+] is always Arg and the alternatives such as Cys-n instead of n-Ser, and Gly-Gly-n preceding the 2nd charge are specific for PUMPs.

The 4th transmembrane segment starts at the matrix interface by one free residue followed by the Leu-Trp-[+]-Gly sequence that exists as Leu/Phe-ϕ-[+]/Gln(Ser)-Gly in MACPs and contains well conserved Gly. The next OH (Thr-Thr or Thr-Ser) doublet in UCP1 and UCP2 is altered by Trp, Leu or Gly in other UCPs. The next 16 residues of the 4th transmembrane segment form a homologous motif that starts with conserved Pro178 and contains one conserved negative charge, plus Arg182 in all UCPs but bovine UCP1, and 5 semiconserved residues in UCP subfamily:

Pro-Asn/Thr-n-X-[+]-Asn/Ser/Ala-n-Ile/Leu-n-Asn/Val-Cys/n-n/Thr-[–]-n-n/Thr/Pro-OH/Val.

We can define it as a 3rd UCP signature (4th transmembrane segment). The last residue is Thr or Ser (Val in BMCP1, that contains Pro prior to it), [+] is always Arg and [–] is Glu.

Conclusion

We have found several regions in UCP sequence, which have common character in UCPs, but are not present in other MACPs. We chose several residues from the 1st transmembrane and the 2nd matrix UCP signatures for the site-directed mutagenesis and characterized properties of respective UCP1 mutants (see the next chapter).

Figure 2 Alignment of uncoupling protein sequences as compared to the yeast dicarboxylate carrier (DTP) sequence and majority sequences of ADP/ATP carrier and phosphate carrier.

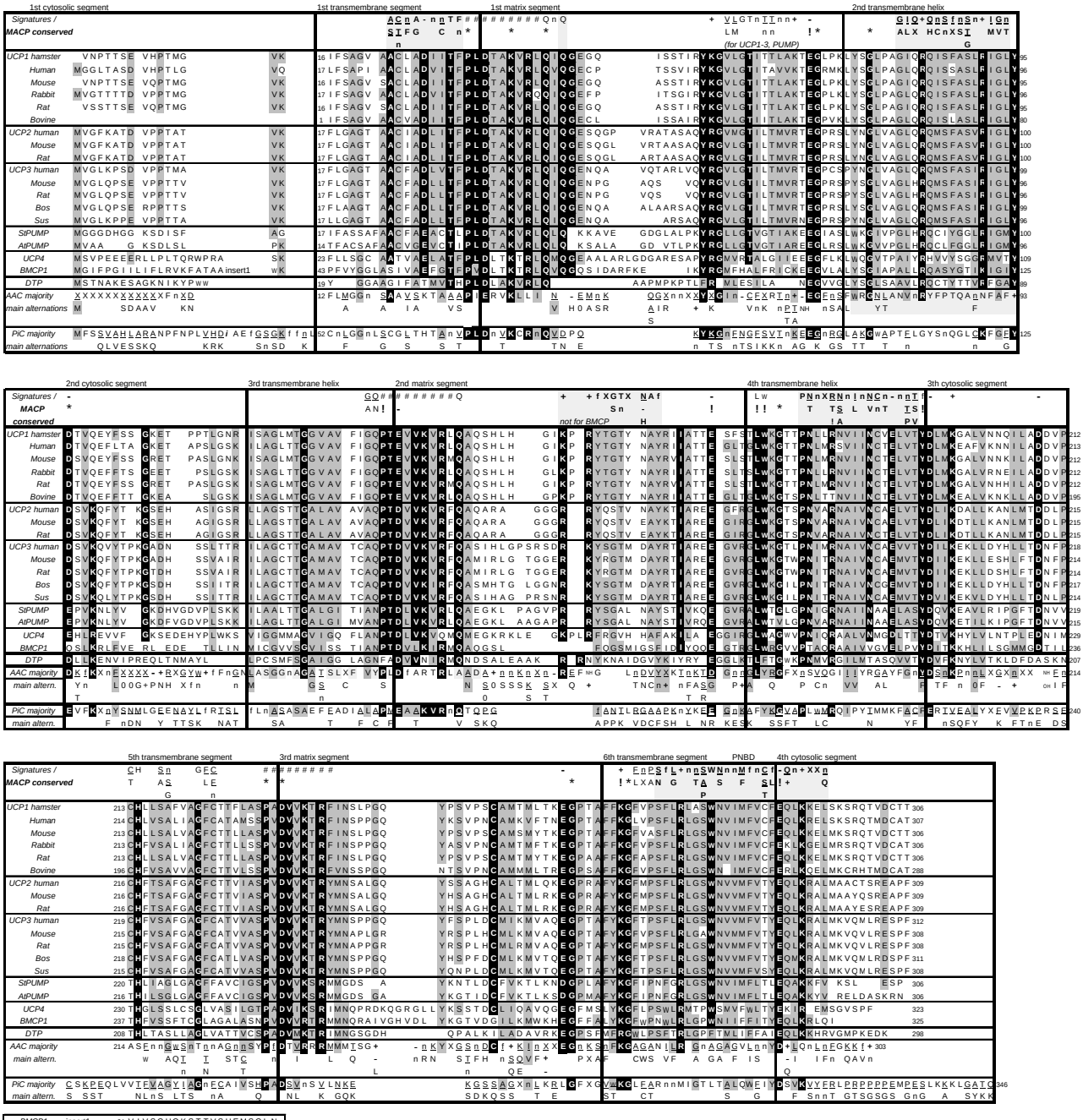

The absolutely conserved residues and charges in UCPs are white in *black boxes*, the semiconserved residues (at least in 3 UCPs) are *shadowed*. The MACP-signatures are marked by #, the defined UCP-signatures are written above as consensus sequences (*dotted background*; f stands for aromatic residue, other symbols see text). *Stars* depict the residues well conserved in the MACP family members (up to 10 exceptions); exclamation marks refer to the "quite conserved" residues (from 10 to 20 exceptions). Majority sequences of AAC and P_iC are based on the prevailing residues (with the most frequent alternatives listed in the row below) among 19 and 6 sequences of different species of AAC and P_iC, respectively. Unique AAC sequences are outlined by the dotted background. The transmembrane regions are considered according to Klingenberg [28]. The alignment was performed using the clustal method (Megalign program from the Lasergene 99 sequence analysis system, DNASTAR).

EXPERIMENTAL PART

UCP1 and its mutants

In this chapter, the analysis of transport properties of several mutants of UCP1 is shown. The transport mediated by UCP1 (mutants) was measured in proteoliposomes, using fluorescent probe, SPQ, to detect the concentration changes of the ions studied - protons and chlorides. We characterized properties of UCP1 mutants, mutated in two important regions - the first group of mutated amino acid residues belonged to the "1st UCP-specific transmembrane motif". We studied mutants D27V, T30A and the triple-mutant C24A-D27V-T30A. The second group belonged to the second matrix loop - we tested the double mutant H145L-H147L and R152L, located in the "UCP-signature".

Figure 3 Amino acid residues of UCP1 mutated in this work. The model of transmembrane spanning of UCP1 is drawn with indicated AARs mutated (small elipses). Black regions indicate the UCP-signatures. The transmembrane segments are represented by cylinders 1-6. AARs at the interface of the membrane are indicated by their sequence position numbers.

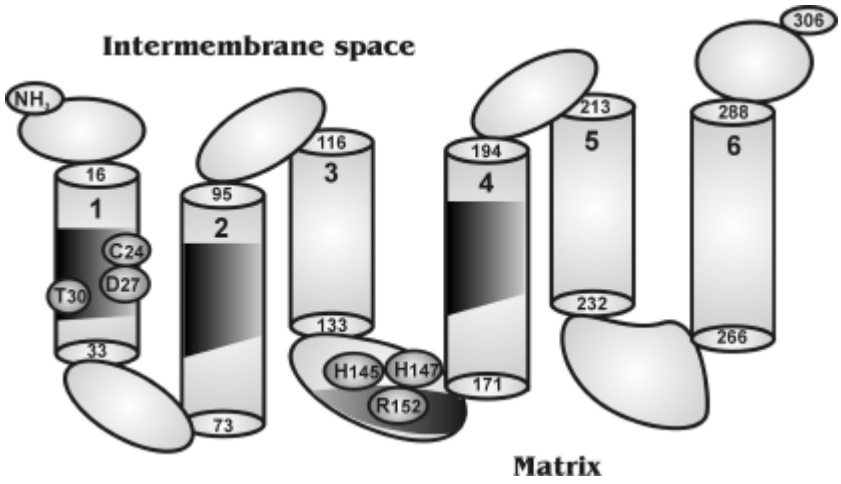

Methods

Rat UCP1 gene placed under the control of galactose promotor in the shuttle *(Sacharomyces cerevisiae/Escherichia coli*) vector pCGS 110 was PCR-amplified in the elongation process starting from two antiparallel primers carrying codon for alanine in place of original threonine. Vectors were proliferated in *E. coli* host, plasmid DNA was isolated and sequenced.[1] Selected clones were electroporated into *S. cerevisiae* yeast and UCP1 expression was stimulated by addition of galactose. The isolation of yeast mitochondria followed in principle the same method as [36] with minor changes.

Reconstitution of UCP1 into proteoliposomes and measurement of proton and chloride transport

I followed the method, originally based upon Klingenberg's protocol [30], adopted for fluorescent probes by Dr. Ježek [23], [19],[24] and in [37]. The fluorescent probe SPQ was used for the measurement of H^+ efflux and Cl^- uptake to liposomes.

The fluorescence was measured on the spectrofluorophotometer Shimadzu RF-5301PC, with Xenon lamp as an excitation source. SPQ fluorescence was excited at 340 nm (10 nm band-pass) and the signal collected at 444 nm (5 nm band-pass). The proton transport was detected via changes in SPQ fluorescence after addition of valinomycin. Typically, in the 10th second, a fatty acid was added. In the 30th second, valinomycin was added (final concentration 0.1 μM), which triggered the H^+ transport. The calibration of

[1] The site-directed mutagenesis was done by Mgr. Petr Hanák.

fluorescence signal was done according [23], [24]. When analyzing kinetic data of the transport, I used Michaelis-Menten formalism.

For the measurement of binding of ^{3}H-GTP to UCP1 mutants, we adopted the anion-exchange method of Klingenberg [31] and measured GTP binding to UCP1 mutants.[2] The protein content was measured by the Amido Black method, described in [27].

Results and discussion

The proton and chloride leaks

The proton and chloride leaks under different conditions (± laurate, ± K^+ diffusion potential) were measured. The comparison of the proton leak and an example of UCP1-induced proton flux is shown at the Figure 4.

Figure 4 Different types of H^+ leak in comparison with UCP1-induced H^+ efflux.

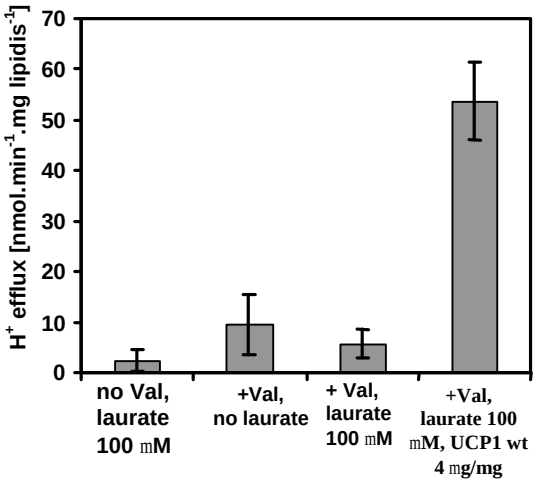

The resembling permeability coefficient for proton leak in the presence of K^+ diffusion potential is 8.5 $.10^{-4}$ cm.s^{-1}, which is a bit higher, than presented in literature under similar conditions (1.4 $.10^{-4}$ cm.s^{-1} [8]). If we calculate the chloride permeability coefficient from Cl^- leak observed in the absence of K^+ diffusional potential (? Cl^- 215 mM), we get the value **(1.63 ± 0.5).10^{-10} cm.s^{-1}**. The Cl^- leak in the presence of K^+ diffusional potential (up to 8 nmol.min^{-1}.mg lipids^{-1}) was higher than observed values 4 nmol.min^{-1}.mg lipids^{-1} [23] or 1.2 nmol.min^{-1}.mg lipids^{-1} [36], but the ? K^+ used in our experiments was also higher (215 mM vs. 150 mM).

The proton and chloride transport mediated by UCP1 mutants and its kinetics

In order to exclude the influence of non-specific proton leaks, the proton transport was analyzed by the means of the dependence of H^+ flux J-J_0 (in nmol.min^{-1}) on the protein concentration in liposomes. From this dependence, the protein-dependent part of H^+ flux, R (in nmol.min^{-1}mg prot.$^{-1}$), and the protein-independent part of the flux, R_0 (in nmol/min) were separated according to the linear regression of Eq. 2

$$\textbf{Eq. 2} \quad J - J_0 = R.[protein](mg) + R_0$$

Linear regression of this dependence for wild-type UCP1 yielded ~ 13.5 μmol.min^{-1}.mg prot^{-1}, corresponding to 15 s^{-1} turnover per dimer (Figure 5b).

UCP1 mutants (except of T30A) exhibited quite flat dependence on the protein amount. Namely the triple UCP1 mutant C24A-D27V-T30A showed no dependence of H^+ flux on the protein content. Typical

[2] The method was introduced to our laboratory by Dr. Eva Škobisová.

examples of H^+ efflux for wild type UCP1 and C24A-D27V-T30A mutant are shown at Figure 5b. As the H^+ efflux was independent on protein content of C24A-D27V-T30A mutant, the curves shown resemble the H^+ leak caused mainly by cycling of lauric acid via laurate-valinomycin complexes.

Figure 5 a) Lauric acid- induced H^+ uniport as a function of incorporated protein for various UCP1 mutants. Rates of H^+ efflux induced by 100 μM lauric acid in the presence of 0.1 μM valinomycin are plotted *vs*. the protein-to-lipid ratio (in μg protein per mg lipid). **Full diamonds**: wild-type UCP1; **open diamonds**: T30A mutant; **open squares**: R152L mutant; **full triangles**: D27V mutant; **open rings**: H145L-H147L mutant; **full rings**: C24A-D27V-T30A mutant. **b) Typical runs of H^+ efflux in the presence of 50 mM lauric acid shown for UCP1 wild type (wt) and C24A-D27V-T30A mutant.** Runs in the presence of 2.5 mM external ATP are shown (grey lines).

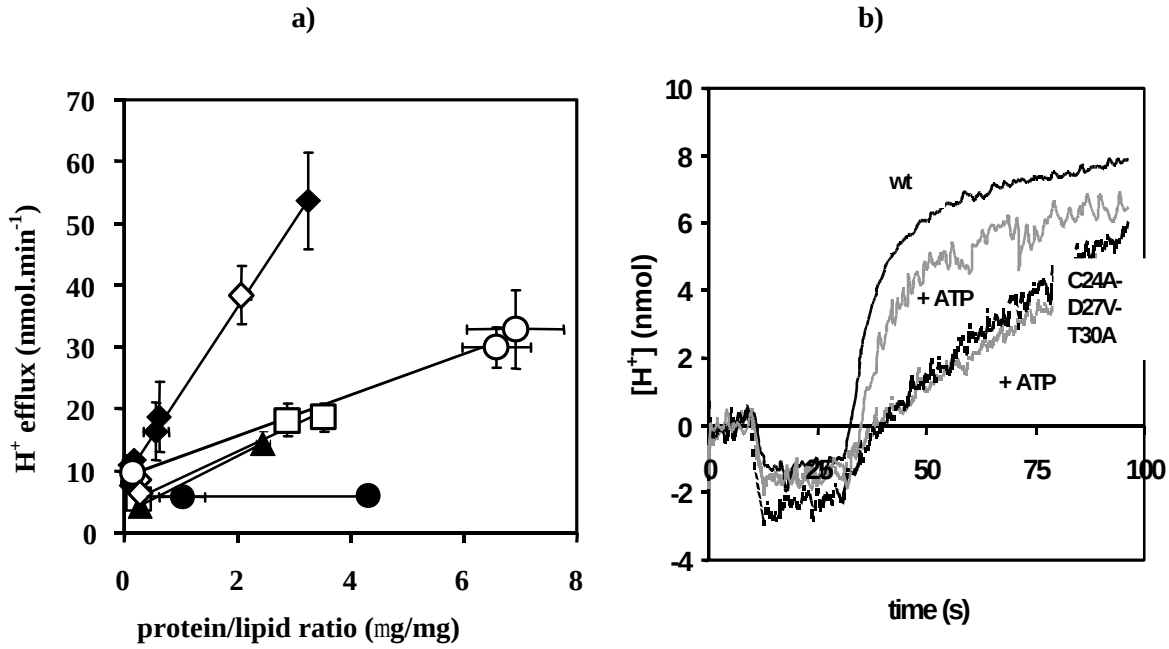

Other characteristics of studied mutants can be provided by the H^+ uniport kinetics. The kinetic data also indicated the reduced ability to mediate FA-induced H^+ uniport for all studied mutants but T30A. Figure 6a shows the direct kinetic plots..

The derived V_{max} values are reduced nearly to half for the D27V and R152L mutants, to ~30% for the H145L-H147L mutant and to zero for the C24A-D27V-T30A mutant (Table 1). The apparent K_ms for these mutants were 2 to 4 times higher (K_m for the triple mutant cannot be derived due to zero approaching fluxes). Consequently, the apparent affinity of these mutants for lauric acid is much lower. This affinity was ~2.5 times lowered also for the T30A mutant even when the V_{max} value was not reduced (Table 1).

Figure 6 a) Direct kinetic plots for lauric acid- induced H^+ uniport in proteoliposomes containing various UCP1 mutants. Rates of H^+ uniport (efflux) *per* mg protein are plotted *v.s.* total concentration of lauric acid used for uniport induction in the presence of 0.1 μM valinomycin. Rates of non-protein dependent transport ("H^+ leak"), taken as intercepts of protein dependencies for each FA concentration such as shown in were subtracted from all the data. **Full diamonds**: wild-type UCP1; **open diamonds**: T30A mutant; **open squares**: R152L mutant; **full triangles**: D27V mutant; **open rings**: H145L-H147L mutant; **full rings**: C24A-D27V-T30A mutant. **b) Cl^- uniport in proteoliposomes containing various UCP1 mutants.** Rates of Cl^- uptake induced by 1 μM valinomycin are plotted *vs.* external Cl^- concentration for various UCP1 mutants (the same symbols as in the left panel). The scales are the same in order to compare the transport rates for H^+ and Cl^-.

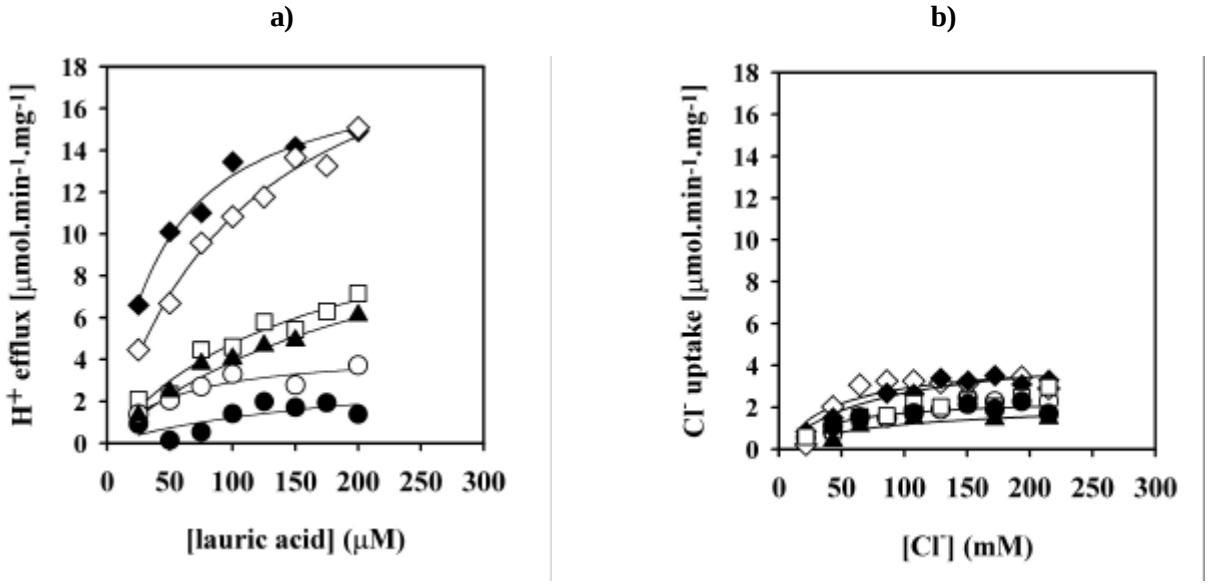

Table 1 Kinetic parameters for H^+ and GTP dissociation constants for various UCP1 mutants. Standard errors refer to the linear regressions of the data. Ratios are calculated at least from three experiments for each transport mode and mutant.

Mutant	H^+ efflux V_{max} ($\mu mol.min^{-1}mg^{-1}$)	H^+ efflux K_m (μM)	K_d of ^{3}H-GTP binding [μM]
Wild type	18 ± 1	43 ± 5	1.6 ± 0.1
R152L	10 ± 1	93 ± 15	1.6 ± 0.4
H145L-H147L	5.6 ±0.9	79 ± 20	1.1 ± 0.3
D27V	11± 2	162 ± 36	1.8 ± 0.7
T30A	22 ± 2	100 ± 10	1.53 ± 0.05
C24A-D27V-T30A	0.2 ± 0.3	n.d.	1.5 ± 0.2

Unlike the protonophoric function, the ability to conduct a slow Cl^- uniport was preserved in all mutants studied as shown by direct kinetic plots (Figure 6, right panel). However, because of a relatively slow transport, the results had a high experimental error. There were no significant differences in the apparent

K_m of the Cl^- uniport, which is quite high in the range of 80-140 mM. The kinetic parameters for UCP1 wt were: v_{max} = 5.4 ± 0.6 μmol.min^{-1}mg^{-1}, K_m = 107 ± 25 mM

The binding of ^{3}H-GTP to UCP1 mutants.

All studied mutants were also assayed for ^{3}H-GTP binding. They all preserved the normal ^{3}H-GTP binding dissociation constant, such as determined for wild type UCP1 (K_d around 1.6 μM, Table 1). The comparison with the data published shows, that our results are within the range of reported K_ds - from 1.05 μM for pH 6.8 [9] to 7.2 μM ([34], pH not stated). Since the nucleotide binding is retained, it is likely that the overall protein structure was intact in all studied mutants.

Discussion of the transport properties of constructed UCP1 mutants

Structure / function relationships of mitochondrial uncoupling proteins, including UCP1, are not completely understood.

The UCP-signature of the 2nd matrix segment exists in all UCPs but BMCP1 (UCP5) [25],[17]. One of its conserved and unique AARs is Arg152 of UCP1. Here we show that the elimination of its positive charge results in ~50% reduction of v_{max} for FA-induced H^+ uniport and of apparent affinity for lauric acid. It is possible, that Arg152 could directly attract the anionic (COO^-) part of the dissociated FA molecule [25].

The second studied region is also located on the 2nd matrix segment, but outside the UCP-signature. For UCP1 it contains a His pair H145, H147. We confirmed the results of Klingenberg's group [3] that the substitution of both His in our H145L-H147L mutant lead to the FA-induced H^+ uniport with v_{max} reduced by 70% and halved FA-affinity, while the Cl^- uniport and ^{3}H-GTP binding were preserved.

The third studied area was the UCP-signature in the 1st transmembrane segment. The previous D27N substitution (*i.e.* neutralization of the only negative charge in this UCP-signature) resulted in a nearly complete elimination of the FA-induced H^+ uniport while the Cl^- uniport was preserved [9]. Although this was later questioned [42], we now confirmed the importance of Asp27 by obtaining ~ 50% reduction of v_{max} for H^+ uniport and by demonstrating the four-times lowered FA affinity for our D27V mutant. On the contrary, H^+ uniport was preserved in our T30A mutant, but it exhibited 2.5-times lower affinity for FA. Hence elimination of hydroxyl group of Thr 30 is not lethal to H^+ uniport. Moreover, we showed that substitution of all three polar AARs of the 1st transmembrane UCP-signature has completely eliminated the FA-induced H^+ uniport, whereas K_d for ^{3}H-GTP binding remained constant. Since we prefer the fatty acid cycling theory as the mechanism of UCP function (reasons for this are discussed in chapter), we consider a "direct" interpretation (Asp27 participation in the H^+ translocation) less likely. It is difficult to imagine, how could a negatively charged residue interact with fatty acid (or other) anion [15].

The alternative interpretation could be that substitutions of Asp27 rather cause conformational change subsequently affecting the phenotype [9].

Flip-flop of fatty acids - theory and experimental results

Internal acidification (IA) was calculated from the fluorescence change occurring immediately after addition of FA (usually lauric acid).

The pH dependence of the internal acidification was also measured for lauric acid (Figure 7). I wanted to analyze this problem a bit deeper and I created a numerical model describing the situation of fatty acid flip-flop and transport of protons by FA-cycling. I extended the model of [26]. All the calculations were made in MS Excell 97.

As a model situation, I chose the simplified system, which consists of two sides separated by the membrane. If we want to relate this model to our experiments with liposomes, than the side 1 represents external medium (which has infinite buffering capacity), the side 2 represents liposomes (defined by the

buffering capacity inside and pH inside). When a certain amount of a fatty acid is added to the side 1, it equilibrates between two membrane sheets and acidifies the side 2.

Figure 7 a) The dependence of the internal acidification on FA content. b) pH dependence of internal acidification of liposomes as compared with the numerical model. The theoretical prediction seems to be qualitatively correct. The quantitative difference is discussed bellow. (c1(0)=75 nmol/μmol lipids, pK=7.6, other parameters same as in this chapter)

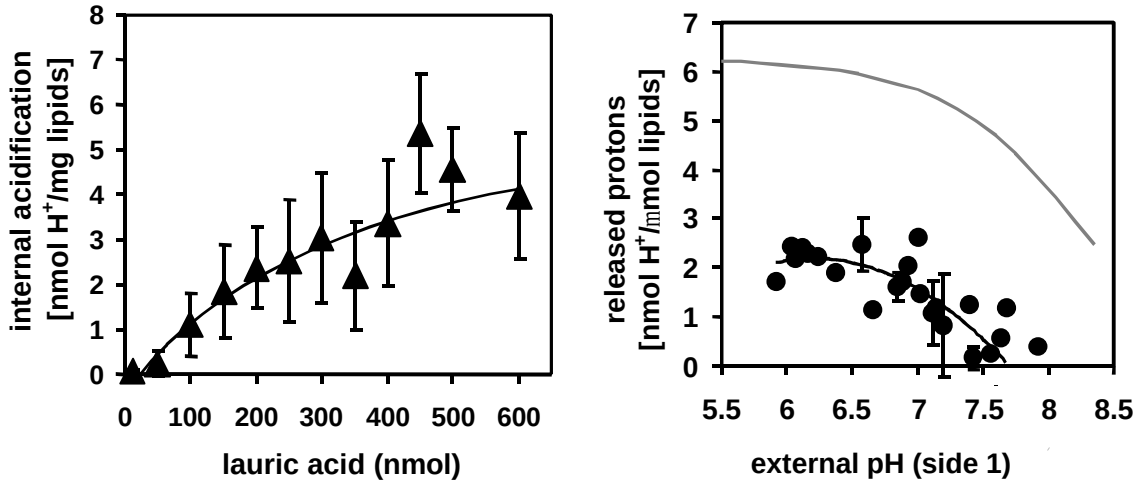

The fatty acid is described by its dissociation constant, pK. I neglected the partitioning of fatty acids into the membrane - all the concentrations used in the model refer to the membrane concentrations. A basic kinetic scheme describing such a case is shown in the Figure 8. I supposed that both transport rates (flip-flop and that of anion back flux) have the same value for both directions of transport. The rate of FA anion back flux may represent either the flip-flop of FA^- (which is known to be very slow) or the rate of transport of FA^- by a protein (e.g. UCP1). The calculations were made under an assumption that the (de)protonation reactions of FA are extremely fast, so that FA^- and FA.H are at either side of the membranes always at equilibrium (this assumption is applied also in the analysis in [26].

Figure 8 The kinetic diagram describing behaving of a fatty acid in the lipid membrane. The situation when $pH_1<pH_2$ is depicted.

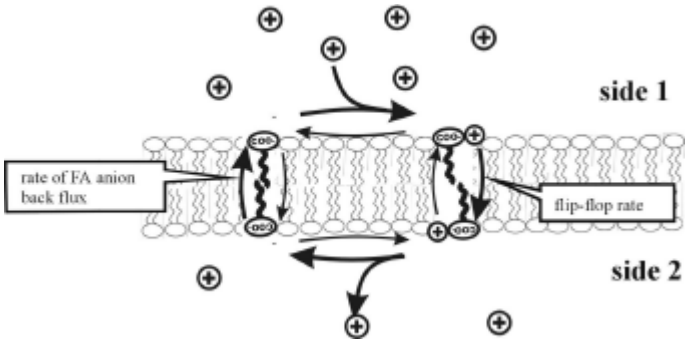

The transport of FA^- creates a charge disbalance between the both sides of the membrane. This fact was taken into account and involved into my calculations as the membrane potential, ? .

The observed quantitative differences between the measurement and the model (Figure 7b) can be explained by an unknown influence of the surface potential (caused by negatively charged lipids and probably also by FA itself) and by the neglecting of the unstirred layer effect.

Measurement of conductivity of planar lipid bilayer membranes with incorporated UCP1

The studying of protein-induced transmembrane transport in planar lipid membranes has several advantages in comparison with (for UCP1 most often) measurement in proteoliposomes; mainly the avoiding of using ionophores for indroducing the membrane potential and access to both sides of the planar membrane. Our aims were to develop an appropriate method to reconstitute UCP1 into planar lipid membrane and than to measure the proton conductivity in the presence of fatty acids.

Methods

There are several ways, how to form a planar lipid bilayer. Two principal strategies exist: i) vesicle-bilayer fusion (where proteoliposomes are fused to preformed planar lipid membranes) and ii) direct formation of planar bilayers from proteoliposomes [47]. I used the second one, which is based on the fact, that monolayers form spontaneously in the air-water interface of any vesicle suspension. These monolayers can be combined either within an aperture in a thin Teflon septum (septum-supported vesicle-derived bilayer) or a glass pipette is used to bring two monolayers into bilayer contact. I used the former method and followed the strategy described in [47], in modifications described in [40].

UCP1 was reconstituted into proteoliposomes directly from BAT mitochondria (slightly modified method as described in [30], [23]) just prior to experiment.

Current-voltage (V-A) characteristics were measured by a patch-clamp amplifier (GeneClamp 5000, Axon Instruments with headstage CV-5B-100G, specialized for bilayer clamping).

For the measurement of total conductivity, triangular voltage ac signal was applied with frequency 0.04-0.07 Hz, V_{p-p}= 100-180 mV. The obtained I(t) dependencies were filtered (box car filter 1 Hz, Clampfit software from Axon Instruments). The conductivity G was calculated from the linear regression of current-voltage dependence in the region -50 mV to +50 mV.

Proton conductivity was measured after applying the pH gradient across the membrane (usually 0.4 pH units). The capacitive current (I_c) was subtracted from the total current and linear fits were calculated in the range from -50 mV to 50 mV. Thus, I got V-A characteristics before and after the application of pH gradient across the membrane and the potential shift V_0 could be estimated. The H^+/OH^- conductance was then calculated according [12].

The proton turnover numbers (number of protons transported by UCP1 dimer per 1s) were calculated according the equation

$$\textbf{Eq. 3} \quad Turnover[s^{-1}] = \frac{G_{H/OH}.V.3.85.10^6}{protein}$$

where $G_{H/OH}$ [$S.cm^{-2}$] is the proton conductivity, V =180 mV and 'protein' is the protein content in μg of protein per mg of lipids.

Results and discussion

The average value of capacity (per membrane area) was **0.89 ± 0.08 μF/cm²** (0.6-1.2 μF/cm²). It did not depend either on protein content, or on fatty acid content. The average conductivity of planar membranes without oleic acid was **$(1.4 . 10^{-8} \pm 0.6 . 10^{-8})S.cm^{-2}$**, independently on the UCP1 content.

The conductivity did not markedly change in the presence of oleic acid (up to 20% weight), which confirms the results of [39]. In the presence of UCP1, the conductivity rise was approximately one order of magnitude. Inhibition by ATP (1.9 mM) was also observed. However, the results were quite scattered, being probably influenced by the history of each planar membrane.

The proton conductivity was measured for 5 independent proteoliposome preparations.

The activity of UCP1 in the lipids used in experiments (mostly *E.coli* polar lipid extract, Avanti) on planar membranes was checked by the SPQ quenching experiment. It seems, that UCP1 is active in mixtures containing *E.coli* lipids, although the results are more or less only qualitative. The turnover numbers measured were around 50 s^{-1} for 5.3 % oleic acid.

Figure 9 V-A relationship of planar lipid membranes - comparison of a membrane containing oleic acid, in the absence of it and in the presence of 1.9 mM ATP**.** The nonlinearity of the V-A characteristics can be explained by the existence of an energy barrier inside the membrane [13].

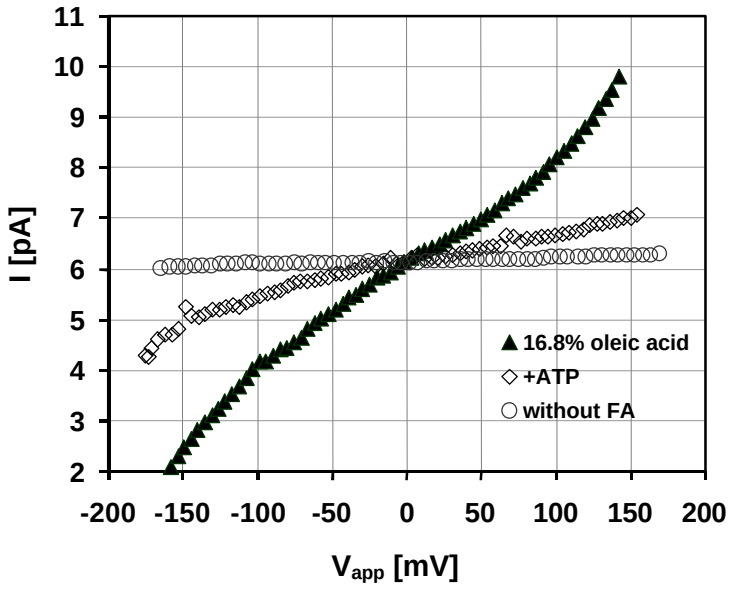

Figure 10 a) The shift of V-A characteristics after applying pH gradient (? pH 0.4) In this case, the observed V_0=14.3 mV gave the transference number of H^+/OH^- 60% (Nernst potential in this case should be 23.8 mV). ? V-A characteristics before and o after the applying of the pH gradient across the membrane. **b) Proton turnover numbers as measured for planar membranes containing 2.5-4.5 mg UCP1 / mg lipids.** The error bars show the average deviation of the measurements done (not true experimental error).

a) **b)**

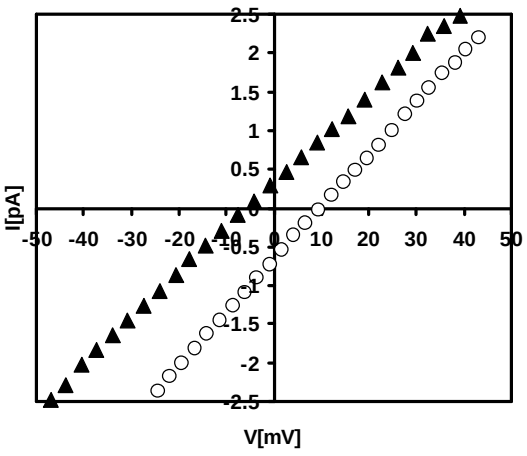

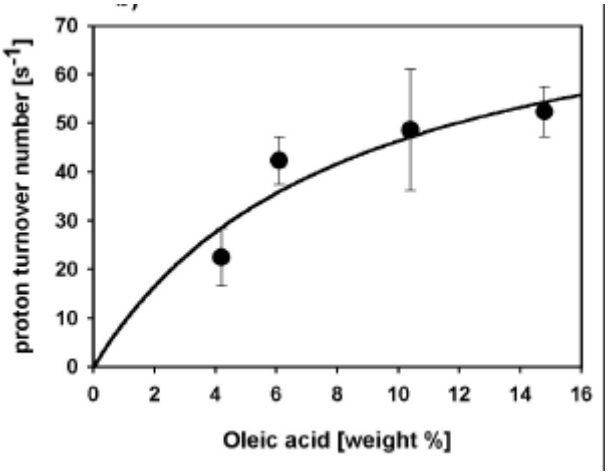

The most important finding of this study is that UCP1 is not active in the absence of fatty acids - the conductivity of planar membranes is not changed in the presence of UCP1. Thus, the results presented here are the confirmation of the absolute requirement of fatty acids for the protonophoric action of UCP1.
It is difficult to compare the transport activities of UCP1 - there are big differences among the published results. The values of proton conductivity as measured on planar membranes are a bit higher[3] (maximal turnover >~ $60s^{-1}$), than the published values ([14], [15], [34]), but comparable with the values obtained by SPQ quenching method measured on the same lipids and with the same fatty acid.

Conclusions

- UCP1 was successfully reconstituted into planar lipid bilayer
- Activity of UCP1 was observed as a change of the overall and proton conductivity of planar membranes. The change of conductivity in the presence of UCP1 and oleic acid was approx. one order of magnitude, the turnover number (calculated for V_{app} 180 mV) was up to 60 s^{-1} per UCP1 dimer for 15 % oleic acid. Activation by oleic acid and inhibition by ATP was observed.
- In the absence of oleic acid, no enhancement of membrane conductivity was observed. The conclusion is that fatty acids are essential for UCP1 to act as a protonophore.

Effects caused by UCP2 and UCP3 in mitochondria

The detection of effects caused by UCP2,3 is very difficult and not so many studies on this theme exist. The reason is probably the low content of UCPn in normal tissues. Possible approaches are either to use transgenic animals as control (with knockout gene for UCPn) or to use transcription regulators of UCPn in order to enhance their content. We tried to detect effects caused by UCP2 directly in isolated liver mitochondria after the treatment by lipopolysaccharide (LPS). Two approaches used - measurement of mitochondrial membrane potential and binding of nucleotides to intact mitochondria - are described in this work.
Moreover, we made the comparison of PN binding to mitochondria of different tissues. However, it is too early to relate them to UCPn, before their real content in respective tissues is known.

Materials and Methods

Wistar rats were injected intraperitoneally 1 mg of LPS (lipopolysaccharide, *E.coli* serotype 055:B5) (female mice C57BL/6 were injected 100 μg of LPS) and killed after 17-18 h for the isolation of mitochondria.
Brown adipose tissue mitochondria (BAT mitochondria) were isolated from brown adipose tissue of syrian hamsters, kept for 2-4 weeks in 4°C. The isolation procedure for BAT, liver and kidney mitochondria followed the protocol described in [6]. For isolation of muscle mitochondria, rat hindlimb skeletal muscle was taken, then cut to small pieces and homogenized. After a centrifugation at 700 g, the supernatant was taken and centrifuged at 10 000 g and 5000 g in order to get mitochondria. The isolation medium was composed of 100 mM sucrose, 100 mM KCl, 50 mM Tris-Cl, 1 mM KPi, 0.1mM EGTA, pH 7.4.

[3] Note however, that oleic acid is a better activator of UCP1-mediated proton transport than lauric acid [164].

Mitochondria – measurement of the membrane potential

In order to measure the mitochondrial membrane potential, I used the fluorescent probe DASPMI (dimethylaminostyrylmethylpyridiniumiodine), a kind of electrochromic styryl dye [2]. Fluorescence measurements were done on Shimadzu RF5000 spectrofluorometer, the excitation wavelength was 465 nm, the emission wavelength 559 nm. For the energization of mitochondria I used succinate (10 mM) as substrate for liver mitochondria. For BAT mitochondria, I took advantage of carnitine cycle (additions of ATP, CoA, carnitine, pyruvate, malate), which depletes mitochondria of fatty acids [20] by their β-oxidation. After obtaining the maximum membrane potential (i.e. maximum fluorescence signal of DASPMI), I added a fatty acid tested. After the stabilization of the resulting lower potential, I added FCCP in order to depolarize mitochondria and to see the fluorescence resembling zero potential.
We defined as "% uncoupled " the ratio between fluorescence decrease induced by tested compounds vs. total fluorescence decrease induced by uncoupler (FCCP). EC_{50} was calculated as

Eq. 4
$$EC_{50} = 10^{-\frac{A}{B}}$$

A and B are parameters obtained from linear regression based on Hill plot, represented by the following equation. A represents Hill coefficient.

Eq. 5
$$\frac{1}{\log(\frac{1}{UNC} - 1)} = A.\log(X) + B$$

As the response of DASPMI is not linear and we did not calibrate it to the membrane potential, EC_{50} values do not reflect the real dose-response curve. Therefore we used it only as a qualitative parameter, for comparison of the results made under the same conditions.

Measurement of nucleotide binding to mitochondria

Mitochondria (approximately 200 µl of 0.8 mg/ml) were incubated with 8-320 pmol of ^{3}H-GTP and then filtered on Millipore nitrocellulose filters (0.45 µm pores) and washed by 1 ml of isolation medium. The assay medium contained 100 mM sucrose, 20 mM HEPES-Tris (pH 7.0), 1 mM EDTA, 2 µM rotenone and 5 µM CAT. The radioactivity of the material remaining on the filter corresponds to number of nucleotide molecules bound to proteins of mitochondrial membranes. For details of calibration and construction of Scatchard plots [44].

Results

The membrane potential

Since it has been known, that lipopolysaccharide can induce expression of UCP2 in liver, it seemed to us, that liver mitochondria could be a good model to study effects of UCP2. I tried to compare the sensitivity of liver mitochondria (from mice, either treated by LPS or not - according [10]) to uncoupling caused by lauric acid. In order to exclude the contributions of AAC and aspartate/glutamate carrier to the uncoupling, CAT and glutamate were present in the assay medium. The dose-response to lauric acid was measured at three values of pH - since it has been published, that the residual uncoupling after subtracting the effects of AAC and aspartate/glutamate carrier depends on pH [42].
The increase in the sensitivity of membrane potential to lauric acid after LPS treatment is only slight, not significant (within the experimental error).

Figure 11 Comparison of dose-responses of relative uncoupling efficiency to lauric acid. Liver mitochondria of mice treated by LPS vs. non-treated ones. The membrane potential was measured by DASPMI, rotenone, oligomycin, CAT and glutamate were added prior to addition of lauric acid. The results were corrected for a spontaneous drop of potential. Full symbols - LPS treated, open symbols - control measurements.

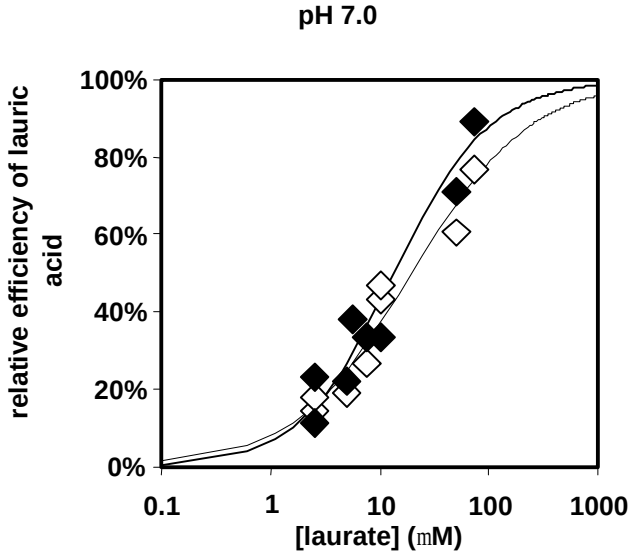

Table 2 EC_{50} [mM] of the dose-responses to lauric acid in mice liver mitochondria.

EC_{50} [mM]	pH 7.0	pH 7.4	pH 7.8
control animal	20 ± 10	29 ± 34	25 ± 11
treated by LPS	14 ± 6	22 ± 17	21 ± 12

Binding of GTP to mitochondria

The binding of GTP to intact liver, lung and kidney mitochondria was assayed on control animals (Wistar rats) and on those treated by LPS. The only tissue, where we detected the change after the LPS treatment, was liver. The observed difference was observable, however, not statistically significant ($p<0.18$, Student's test). This is caused by very weak binding of GTP to mitochondria, which is difficult to measure. Lung and kidney mitochondria did not change their GTP binding properties after LPS treatment.

Table 3 Binding constants and number of binding sites in several kinds of rat mitochondria (± LPS stimulation). Standart errors refer to the linear regressions of the averaged data.

tissue	K_d [μM]	Binding sites pmol/mg	% of mitochondrial protein *
liver	**0.23** ± *0.03*	**21** ± *4*	0.14%
liver + LPS	**0.51** ± *0.08*	**59** ± *14*	0.39%
lung	**0.43** ± *0.03*	**182** ± *18*	1.20%
lung + LPS	**0.47** ± *0.14*	**172** ± *73*	1.14%
kidney	**0.3** ± *0.06*	**74** ± *22*	0.49%
kidney + LPS	**0.24** ± *0.04*	**67** ± *17*	0.44%
muscle (hindlimb)	**0.14** ± *0.02*	**28** ± *6*	0.19%

*weight ratio, based on the assumption that 1 binding site has Mw 66 000 Da.

Figure 12 a) Liver mitochondria : o-not stimulated, ? -stimulated by LPS ; The difference at 240 and 320 pmol GTP has p<0.18 (Student's test). 5 independent experiments were done for both kinds of mitochondria. The number of GTP binding sites rose 2-3x after LPS treatment. **b) Scatchard plot [44] - comparison of mitochondria from different tissues: o lung, ? kidney, · liver,** Ñ **muscle**

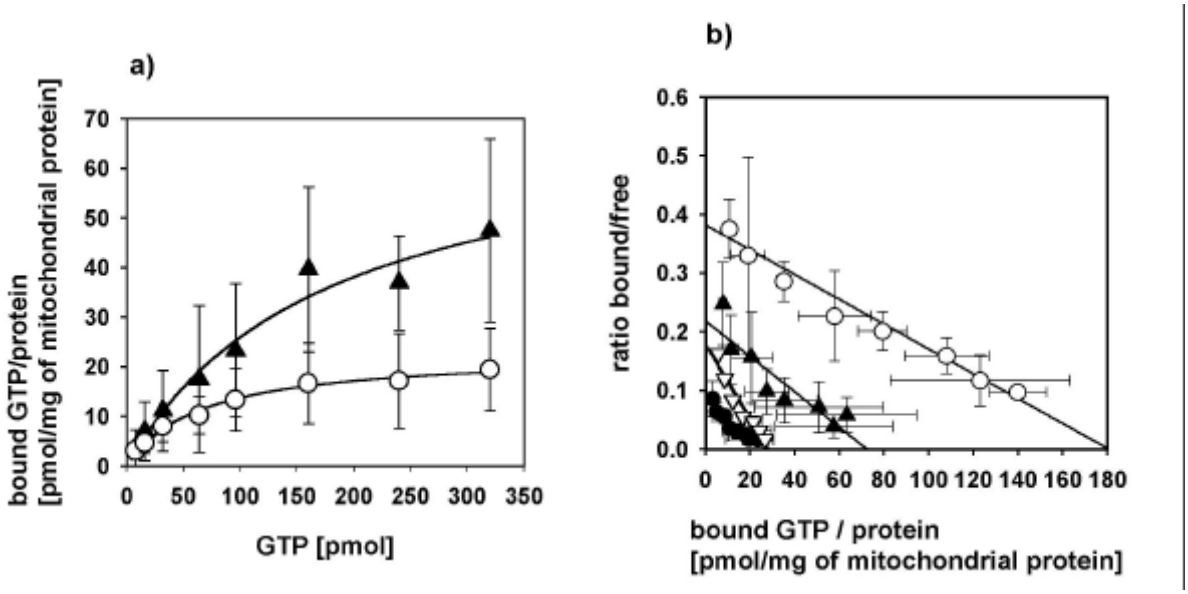

If we compare the tissues studied, the strongest GTP binding exhibited lung mitochondria (182 pmol GTP/mg of mitochondrial protein), followed by kidney, muscle and liver mitochondria. For comparison, BAT mitochondria of cold-adapted animals bind 350-1200 pmol GTP/mg of mitochondrial protein (as reviewed in [16]). Our own observation for hamster BAT mitochondria was ~ 320 pmol GTP/mg of mitochondrial protein (only 1 experiment).

Discussion

There were found only very slight differences (within experimental error) between the uncoupling caused by lauric acid[4] for LPS treated/normal liver mitochondria. This may have several reasons, which cannot be distinguished in the moment:

- UCP2 expression is not significantly increased after LPS treatment; the published results report primarily the rise in UCP2 mRNA, but not the protein itself.
- The amount of UCP2 present in liver after LPS treatment is so low, that its action cannot be detected by the methods used - it may be shielded by the uncoupling action of other MACP.
- The conditions chosen for the experiments were not suitable to detect the UCP2-caused effects - for example fluorescent probes for mitochondrial membrane potential have the highest resolution in the lower potentials [Dr. Vicente, personal communication]. The use of TPP electrode, which is more sensitive at higher values of membrane potential could solve this problem.

Since it is supposed that UCP2,3 also bind purine nucleotides[5], the binding of GTP to intact mitochondria should at least partly reflect the amount of UCP2,3 present there.

---

[4] EC_{50} cannot be related to kinetic parameters, but it reflects qualitatively the sensitivity of mitochondrial membrane potential to fatty acids.

[5] Inhibition by PN observed in [57], reviewed in [81]; binding of GTP to UCP2 measured in our laboratory by Dr. Škobisová, unpublished.

From the studied tissues, lung mitochondria have the highest content of GTP binding sites, kidney and muscle mitochondria follow and the lowest values have liver mitochondria. Without an independent method for estimation of UCP2 content in these tissues, it is impossible to interpret the observed differences. Nucleotides may interact also with other proteins of the inner mitochondrial membrane (e.g. cytochrome c oxidase [41]) and therefore it is not possible to assign all the binding observed only to UCP2-3.

After LPS treatment, we observed the increase in liver mitochondria, but not in lung or kidney mitochondria. If we suppose, that the a GPT-binding unit has the molecular weight 66 kDa, the rise in the number of GTP-binding units observed after LPS-treatment resembles 0.25% of mitochondrial protein. For comparison, UCP1 may represent 2.4% or more [11]. As the binding of GTP to liver mitochondria is very low, experimental errors are quite high and the observed increase after LPS treatment is not statistically significant.

The increase of UCP2 mRNA in liver is reported in several articles ([7] for rats, [10] for mice), but the increase of the protein level itself was denied in [38] (based on the detection by anti-UCP2 antibodies). Our results oppose the results of [38], since there was observed constant level of UCP2 in liver and rise in the level of UCP2 in lung after LPS treatment. We observed the difference in GTP binding in liver mitochondria and not in lung mitochondria after LPS treatment.

CONCLUSION

Here, I would like to summarize the results achieved during my work on the thesis.

(1.) Having compared the known sequences of UCPs and some of their relatives from the MACP family, we have identified **common sequence motifs** in the 2nd matrix and in the 1st, 2nd and 4th transmembrane segments of UCPs, that in principle do not exist in the other carriers of the MACP gene family. Consequently, we defined them as **"UCP-signatures"**.

(2.) When constructing several mutants of UCP1, we focused on the polar and charged residues of the three parts of UCP1 - from the UCP signatures (in the 1st transmembrane segment and in the 2nd matrix segment) and the histidine pair located in the 2nd matrix segment.
The proton and chloride transport of the mutants was measured in proteoliposomes with the help of SPQ fluorescent probe ('SPQ quenching method'). For mutants D27V and H145L-H147L, we confirmed the results published previously [4], [9]. The transport properties of wt UCP1 were in agreement with the values published [23], [19], [14], [15]. The binding of GTP was evaluated by the anion-exchange method.
All mutants transported chloride and bound GTP in a similar extent as wt UCP1. However, **in the proton transport were found following differences**:

- The triple mutant C24A-D27V-T30A did not transport protons at all.
- In D27V, R152L, and H145L-H147L, v_{max} of proton transport was reduced at least to 50%.
- The affinity for lauric acid (K_m) was reduced in D27V, R152L, T30A, and H145L-H147L.

We speculate, that R152 could interact with fatty acids.

(3.) The simplified model describing the behaviour of fatty acids in the liposomal membrane was developed. Although it gives reasonable qualitative predictions, the values of internal acidification differ from those observed experimentally. The possible reasons for the difference were discussed.

(4.) Proton and chloride leaks under the conditions of the SPQ quenching experiment were evaluated.

(5.) UCP1 was successfully **reconstituted into planar membranes** and the changes in the conductivity (total and proton conductivity) were measured in the presence of oleic acid. The activity of UCP1 calculated from changes in proton conductivity is similar to the results obtained elsewhere [14].
Fatty acids (oleic acid) were confirmed to be necessary activators of UCP1-mediated transport, since the conductivity of planar membranes with incorporated UCP1 was not increased in the absence of oleic acid.

(6.) In the search for detecting the effect of UCP2 and UCP3 **- response of the membrane potential** (? ?) **to fatty acids and binding of GTP to mitochondria** were studied.
In liver mitochondria of animals treated by LPS, no significant changes in the response of ? ? to laurate were observed at pH 7.0-7.8. The binding of GTP was studied for lung, kidney and liver mitochondria. The increase of the number of GTP binding sites after LPS treatment was observed only for liver mitochondria (the change resembling 0.25% of total mitochondrial protein).

REFERENCES

1 Aquila,H., Link,T.E., Klingenberg,M. (1987) FEBS Lett. 212: 1-9

2 Bereiter-Hahn,J. (1976) BBA 423: 1-14

3 Bienengraber, M., Echtay,K.S., Klingenberg,M. (1998) Biochemistry 37: 3-8

4 Bienengraeber,M., Echtay,K.S., Klingenberg,M. (1998) Biochemistry 37: 3-8

5 Boss,O., Samec,S., Paoloni-Giacobino,A., Rossier,C., Dulloo,A., Seydoux,J., Muzzin,P., Giacobino,J.P. (1997) FEBS Lett. 408: 39-42

6 Cannon,B., Lindberg,O. (1979) in Methods Enz. 55: 65-78

7 Cortez-Pinto,H., Yang,S.Q., Lin,H.Z., Costa,S., Hwang,C.S., Lane,M.D., Bagby,G., Diehl,A.M. (1998) Bioch. Biophys. Research communications 251: 313-319

8 Deamer,D.W.: Proton permeation of lipid bilayers (1987) J. Bioenergetics and Biomembranes 19: 457-479

9 Echtay,K.S., Winkler,E., Bienengraeber,M., Klingenberg,M. (2000) Biochemistry 39: 3311-3317

10 Faggioni,R., Shigenaga,J., Moser,A.,Feingold,K.R., Grunfeld,C. (1998) Bioch. Biophys. Research communications 244: 75-78

11 Feil,S., Rafael,J. (1994) Eur. J. Biochem. 219: 681-90

12 Fuks,B., Homble,F. (1994) Biophys. J. 66: 1404-1414

13 Garlid, K.D., Beavis,A.D., Ratkje,S.K. (1989) BBA 976: 109-120

14 Garlid,K.D., Jaburek,M., Ježek,P., Varecha,M. (2000) BBA 1459: 383-389

15 Garlid,K.D., Orosz,D.E., Modrianský,M., Vassanelli,S., Ježek,P. (1996) J. Biol. Chem. 271: 2615-2620

16 Hackenberg,H., Klingenberg,E.M. (1980) Biochemistry 19: 548-555

17 Hanák,P., Ježek,P. (2001) FEBS Lett. 495: 137-141

18 Jaburek,M., Varecha,M., Ježek,P., Garlid,K.D: (2001) J. Biol. Chem. 276: 31897-31905

19 Ježek,P., Garlid, K.D. (1990) J. Biol. Chem. 265: 19303-19311

20 Ježek,P., Krasinskaya,I.P., Smirnova,I., Drahota,Z. (1989) FEB 243: 37-40

21 Ježek,P., Modrianský, M., Garlid,K.D. (1997) FEBS Lett. 408: 166-170

22 Ježek,P., Modrianský,M., Garlid,K.D. (1997) FEBS Lett. 408: 161-165

23 Ježek,P., Orosz,D. E., Garlid, K.D. (1990) J. Biol. Chem. 265: 19296-19302

24 Ježek,P., Orosz,D.E., Modrianský,M., Garlid,K.D. (1994) J. Biol. Chem. 269: 26184-26190

25 Ježek,P., Urbánková,E. (2000) IUBMB-Life 49: 63-70

26 Kamp,F., Hamilton,J.A. (1993) Biochemistry 32: 11074-11086

27 Kaplan,R.S., Pedersen, P.L. (1985) Anal. Biochem. 150: 97-104

28 Klingenberg, M. (1990) TIBS 15: 108-112

29 Klingenberg,M., Echtay,K.S. (2001) BBA 1504: 128-143

30 Klingenberg,M., Winkler,E. (1985) EMBO J. 4: 3087-3092

31 Klingenberg,M. (1988) Biochemistry 27: 781-791

32 Mao,W., Yu,X.X., Zhong,A., Li, W.,, Brush,J., Sherwood,S.W., Adams,S.H., Pan,G. (1999) FEBS Lett. 443: 326-330

33 Mitchell,P. (1976) Biochemical society transactions 4: 398-430

34 Modrianský,M, Murdza-Inglis,D.L., Patel,H.V., Freeman,K.B., Garlid,K.D. (1997) J. Biol. Chem. 272: 24759-24762

35 Moualij,B., Duyckaerts,C., Lamotte-Brasseur,J., Sluse,F.E. (1997) Yeast 13: 573-581

36 Murdza-Inglis,D.L., Patel,H.V., Freeman,K.B., Ježek,P., Orosz,D.E., Garlid,K.D. (1991) J. Biol. Chem. 260: 11871-11876

37 Orosz,D.E., Garlid,K.D. (1993) Anal. Biochem. 210: 7-15

38 Pecqueur,C., Alves-Guerra,M.C., Gelly,C., Lévi-Meyrueis,C., Couplan,E., Collins,S., Ricquier,D., Bouillaud,F., Miroux,B. (2001) J. Biol. Chem. 276: 8705-8712

39 Pohl,E.E., Peterson,U., Sun,J., Pohl,P. (2000) Biochemistry 39: 1834-9

40 Pohl,P., Saparov,S.M., Borgnia,M.J., Agre,P. (2001) Proc. Natl. Acad. Sci. USA 98: 9624-9629

41 Rohdich, F., Kadenbach,B. (1993) Biochemistry 32: 8499-8503
42 Samartsev,V.N., Mokhova,E.N., Skulachev,V.P. (1997) FEBS Lett. 412: 179-182
43 Sanchis, D., Fleury,C., Chomiki,A., Goubern,M., Huang, Q., Neverova,M., Gregoire,F., Easlick,J., Raimbault,S., Levi-Meyrueis,C., Miroux,B., Collins,S., Seldin,M., Richard,D., Warden,C., Bouillaud,F., Ricquier,D. (1998) J. Biol. Chem. 273: 34611-34615
44 Scatchard,G. (1949) Ann. NY Acad. Sci. 51: 660
45 Several reviews collected in a special chapter: Mitochondria make a comeback (1999) Science 283: 1475-1504
46 Scheffler,I.E. (2000) Mitochondrion 1: 3-31
47 Schindler, H. (1989) in Methods Enz. 171: 225-253
48 Skulachev,V.P. (1991) FEBS Lett. 294: 158-162
49 Walker,J.E., Runswick,M.J. (1993) J. Bioenergetics and Biomembranes 25: 435-446
50 Walker,J.E.: (1992) Curr. Opin. Struct. Biol. 2: 519-526

LIST OF PAPERS

Original articles:

Ježek,P., Urbánková,E.: Specific sequence motifs of mitochondrial uncoupling proteins (2000) IUBMB Life 49: 63-70

Urbánková,E., Hanák,P., Škobisová,E., Ružicka,M., Ježek,P. : Substitutional mutations in the uncoupling protein-specific sequences of mitochondrial uncoupling protein UCP1 lead to the reduction of fatty acid-induced H^+ uniport (2002) International Journal of Biochemistry & Cell Biology 1363: 1-9, in press

Posters:

Urbánková E., Ježek,P. : Specific sequence motifs of mitochondrial uncoupling proteinsu 2nd Colloquium on Mitochondria and Myopathies in Halle-Saale, March 2000

Aleksakhina,K., Urbánková,E., Ježek,P. : Studies of fatty acid-induced uncoupling in the mitochondria from different tissues; FEBS course, Moscow, September 2001

Ježek,P., Urbánková,E., Pohl,E.E., Pohl,P.: Reconstitution of mitochondrial uncoupling protein UCP1 into bilayer lipid membrane, IUPAB meeting, Buenos Aires, April 2002

Ružicka,M., Šantorová,J., Urbánková,E., Škobisová,E., Modrianský,M., Ježek,P.: Lipopolysaccharide and TNF-α-stimulation of UCP2 in rat liver and hepatocytes, EBEC meeting, Arcachon, France, September 2002